

# Entanglement degradation in the solid state: interplay of adiabatic and quantum noise

B. Bellomo,<sup>1</sup> G. Compagno,<sup>1</sup> A. D'Arrigo,<sup>2</sup> G. Falci,<sup>2</sup> R. Lo Franco,<sup>1</sup> and E. Paladino<sup>2</sup>

<sup>1</sup>*CNISM & Dipartimento di Scienze Fisiche ed Astronomiche,  
Università di Palermo, via Archirafi 36, 90123 Palermo, Italy*

<sup>2</sup>*Dipartimento di Metodologie Fisiche e Chimiche, Università di Catania,  
viale A. Doria 6, 95125 Catania, Italy & CNR-IMM MATIS*

(Dated: June 4, 2018)

We study entanglement degradation of two non-interacting qubits subject to independent baths with broadband spectra typical of solid state nanodevices. We obtain the analytic form of the concurrence in the presence of adiabatic noise for classes of entangled initial states presently achievable in experiments. We find that adiabatic (low frequency) noise affects entanglement reduction analogously to pure dephasing noise. Due to quantum (high frequency) noise, entanglement is totally lost in a state-dependent finite time. The possibility to implement on-chip both local and entangling operations is briefly discussed.

PACS numbers: 03.65.Ud, 03.65.Yz, 03.67.Lx, 85.25.Hv

Over the last decade, considerable progress has been made towards the implementation of an electrically controlled solid-state quantum computer. In particular, superconducting high-fidelity [1, 2] single qubit gates with coherence times of about  $1\mu s$  are nowadays available [3, 4]. The possibility to implement two-qubit logic gates has been proved in different laboratories [5] and Bell states preparation has been demonstrated [6]. Recently, highly entangled states with concurrence up to 94 per cent have been generated “on demand” in a circuit quantum electrodynamic architecture, opening the way to the implementation of quantum algorithms with a superconducting quantum processor [7].

In order to achieve the high performances required to overcome classical processors, it is important to establish how long a sufficient degree of entanglement can be maintained in noisy nanocircuits. Implications are the possibility to store entangled states in solid-state memories and entanglement preservation during local operations in quantum algorithms [8, 9]. Solid state noise may represent a serious limitation towards this goal. Superconducting nanodevices are usually affected by broadband noise. Typical power spectra display a  $1/f$  low-frequency behavior followed by a white or ohmic flank [10, 11].

The effects on single-qubit gates of low- and high-frequency noise components are quite different. Adiabatic (low frequency) noise typically leads to power-law decay, quantum (high frequency) noise to exponential behavior [10, 12]. On the other hand, disentanglement may markedly differ from the single qubit decoherence. For instance, at zero temperature, single qubit exponential decay due to a Markovian bath contrasts to finite-time bipartite entanglement degradation, known as “Entanglement Sudden Death” (ESD) [13]. In structured environments non-Markovian noise appears to be more fundamental [14, 15]. Extending the current research on ESD into physically relevant non-Markovian situations remains a challenge [9]. The analysis of entanglement degradation under the simultaneous presence of adiabatic and quantum noise places in this context and it may pro-

vide new insights to the exploitation of solid-state nanodevices for quantum information.

In this Communication we address these issues. We consider two non-interacting qubits subject to independent baths with typical solid-state broadband spectra [16]. Entanglement is quantified by the concurrence [17], which is evaluated in analytic form in the presence of adiabatic noise for classes of entangled initial states presently achievable in experiments. We find that adiabatic noise has the same qualitative effect of pure dephasing noise and no ESD occurs for pure initial states. However, due to the interplay with quantum noise, entanglement is lost in a finite time which depends on the initial entangled state. We comment on the sensitivity to experimental imperfections and qubits operating point. The possibility to implement on-chip both local and entangling operations is briefly discussed.

*Model and evolved two-qubit density matrix* – The system, formed by uncoupled qubits  $A$  and  $B$  affected by independent noise sources, is modeled by  $H_{\text{tot}} = H_A + H_B$ . Each qubit is an-isotropically coupled to a noise source

$$H_\alpha = H_{Q,\alpha} - \frac{1}{2}\hat{X}_\alpha\sigma_{z,\alpha}, \quad H_{Q,\alpha} = -\frac{1}{2}\vec{\Omega}_\alpha \cdot \vec{\sigma}_\alpha. \quad (1)$$

Here  $\hat{X}_\alpha$ ,  $\alpha = A, B$ , are collective environmental variables whose power spectra are  $1/f$ ,  $f \in [\gamma_m, \gamma_M]$  and white or ohmic at  $f \geq \tilde{f}$ , where  $\tilde{f} \leq \Omega_\alpha$  ( $\hbar = 1$ ) [10, 11]. According to a standard model, noise with  $1/f$  spectrum can be originated from an ensemble of bistable fluctuators with switching rates  $\gamma$  distributed as  $1/\gamma$  [18]. The physical origin of these fluctuations depends on the specific setup. Both the operating point (the angle  $\theta_\alpha$  between  $z$  and  $\vec{\Omega}_\alpha$ ) and the splittings  $\Omega_\alpha$  are tunable. By operating each qubit at the “optimal point”,  $\theta_\alpha = \pi/2$ , partial reduction of defocusing may be achieved [4, 10].

The two-qubit Density Matrix (DM) elements are evaluated in the computational basis  $\mathcal{B} = \{|0\rangle \equiv |00\rangle, |1\rangle \equiv |01\rangle, |2\rangle \equiv |10\rangle, |3\rangle \equiv |11\rangle\}$ , where  $H_{Q,\alpha}|0\rangle_\alpha = -\frac{\Omega_\alpha}{2}|0\rangle_\alpha$ ,  $H_{Q,\alpha}|1\rangle_\alpha = \frac{\Omega_\alpha}{2}|1\rangle_\alpha$ . Since each “qubit+environment” evolves independently, the time evolution operator of the

composite system is the tensor product of terms corresponding to the two parts. Thus, once the single-qubit dynamics, expressed by the DM elements  $\rho_{ii'}^A(t) = \sum_{ll'} A_{ii'}^{ll'}(t)\rho_{ll'}^A(0)$ ,  $\rho_{jj'}^B(t) = \sum_{mm'} B_{jj'}^{mm'}(t)\rho_{mm'}^B(0)$ , is solved, the evolved two-qubit DM can be evaluated as [14]

$$\langle ij|\rho(t)|i'j'\rangle = \sum_{ll',mm'} A_{ii'}^{ll'}(t)B_{jj'}^{mm'}(t)\langle ll|\rho(0)|l'l'\rangle, \quad (2)$$

where indexes take values 0,1. We consider extended Werner-like (EWL) two-qubit initial states

$$\hat{\rho}^\Phi = r|\Phi\rangle\langle\Phi| + \frac{1-r}{4}I_4, \quad \hat{\rho}^\Psi = r|\Psi\rangle\langle\Psi| + \frac{1-r}{4}I_4, \quad (3)$$

whose pure parts are the one/two-excitations Bell-like states  $|\Phi\rangle = a|01\rangle + b|10\rangle$ ,  $|\Psi\rangle = a|00\rangle + b|11\rangle$ , where  $|a|^2 + |b|^2 = 1$ . The purity parameter  $r$  quantifies the mixedness and  $a$  sets the degree of entanglement of the initial state. In the experiment of Ref. [7] entangled states with purity  $\approx 0.87$  and fidelity to ideal Bell states  $\approx 0.90$  have been generated. These states may be approximately described as EWL states with  $r_{exp} \approx 0.91$ .

For EWL states, the density matrix in the computational basis is non-vanishing only along the diagonal and anti-diagonal (X form) [13]; in this system this structure is maintained at  $t \geq 0$ . The entangled two-qubit dynamics is quantified by concurrence,  $C(t)$  ( $C = 0$  for separable states,  $C = 1$  for maximally entangled states) [17]. For X states  $C_\rho^X(t) = 2\max\{0, K_1(t), K_2(t)\}$  [19],

$$K_1(t) = |\rho_{12}(t)| - \sqrt{\rho_{00}(t)\rho_{33}(t)}, \quad (4)$$

$$K_2(t) = |\rho_{03}(t)| - \sqrt{\rho_{11}(t)\rho_{22}(t)}. \quad (5)$$

The initial value of the concurrence is equal for both the EWL states of Eq. (3) and reads  $C_\rho^\Phi(0) = C_\rho^\Psi(0) = 2\max\{0, (|ab| + 1/4)r - 1/4\}$ . Initial states are thus entangled provided that  $r > r^* = (1 + 4|ab|)^{-1}$ .

Elements of the two-qubit DM in the basis  $\mathcal{B}$  will be obtained via Eq. (2). To solve the single-qubit dissipative dynamics we apply the multi-stage elimination approach introduced in Ref. [12]. Effects of low- and high-frequency components of the noise are separated by putting,  $\hat{X}_\alpha \rightarrow X_\alpha(t) + \hat{X}_\alpha^f$ . Stochastic variables  $X_\alpha(t)$  describe low-frequency ( $1/f$ ) noise, and can be treated in the adiabatic and longitudinal approximation. High-frequency ( $\omega \sim \Omega_\alpha$ ) fluctuations  $\hat{X}_\alpha^f$  are modeled by a Markovian bath and mainly determine spontaneous decay. Therefore, populations relax due to quantum noise ( $T_1$ -type times), which also leads to secular dephasing ( $T_2^* = 2T_1$ -type). Low-frequency noise provides a defocusing mechanism determining further coherences decay.

*Concurrence under adiabatic noise* – The effect of low-frequency noise components is obtained by replacing  $\hat{X}_\alpha \approx X_\alpha(t)$ . In the adiabatic and longitudinal approximation single-qubit populations do not evolve in time,  $\rho_{ii}^\alpha(t) = \rho_{ii}^\alpha(0)$ , where  $i = 0, 1$ . The leading effect of low-frequency fluctuations is defocusing, given within the static-path approximation (SPA),  $\rho_{ij}^\alpha(t) \approx$

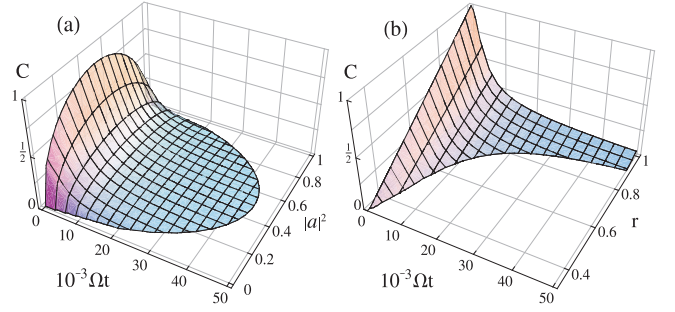


FIG. 1: (Color online) Concurrence (8) at  $\theta = \pi/2$  and  $\Sigma/\Omega = 0.02$ . Panel (a)  $C(t)$  as a function of  $|a|^2$  ( $r = 0.9$ ); Panel (b)  $C(t)$  vs  $r$  ( $a = 1/\sqrt{2}$ ).

$\rho_{ij}^\alpha(0)z_\alpha(t)$  with  $z_\alpha(t) = \int dX_\alpha P(X_\alpha) \exp[-i\omega_{ij}(X_\alpha)t]$ . It amounts to neglect effects of the slow fluctuators dynamics during time evolution. In relevant situations the probability density can be assumed of Gaussian form  $P(X_\alpha) = \exp(-X_\alpha^2/2\Sigma_\alpha^2)/\sqrt{2\pi}\Sigma_\alpha$  and the coherences take the form reported in Ref. [12]. The variance  $\Sigma_\alpha$  can be estimated by independent measurement of the amplitude of the  $1/f$  power spectrum on the uncoupled qubits,  $S_\alpha^{1/f}(\omega) = \pi\Sigma_\alpha^2[\ln(\gamma_M/\gamma_m)\omega]^{-1}$ .

For the initial EWL states of Eq. (3), the concurrences reduce respectively to  $C_\rho^\Phi(t) = 2\max\{0, K_1^\Phi(t)\}$  and  $C_\rho^\Psi(t) = 2\max\{0, K_2^\Psi(t)\}$ , where

$$K_1^\Phi(t) = |\rho_{12}^\Phi(0)||z_A(t)||z_B(t)| - \sqrt{\rho_{00}^\Phi(0)\rho_{33}^\Phi(0)}, \quad (6)$$

$$K_2^\Psi(t) = |\rho_{03}^\Psi(0)||z_A(t)||z_B(t)| - \sqrt{\rho_{11}^\Psi(0)\rho_{22}^\Psi(0)}, \quad (7)$$

give the same concurrence  $C_\rho^\Phi(t) = C_\rho^\Psi(t) \equiv C(t)$

$$C(t) = 2r|ab|\Pi_\alpha \frac{\exp\{-\frac{1}{2}\frac{(c_\alpha\Sigma_\alpha t)^2}{1+(s_\alpha\Sigma_\alpha)^4(t/\Omega_\alpha)^2}\}}{[1+(s_\alpha\Sigma_\alpha)^4(t/\Omega_\alpha)^2]^{1/4}} - \frac{1-r}{2} \quad (8)$$

for times smaller than the adiabatic ESD time,  $t_{ESD}^{ad}$  identified by the condition  $C(t_{ESD}^{ad}) = 0$ . In Eq. (8)  $c_\alpha = \cos\theta_\alpha$ ,  $s_\alpha = \sin\theta_\alpha$ . Adiabatic noise in the longitudinal approximation leads to the same qualitative behavior obtained for pure dephasing noise [13], i.e. the concurrence does not vanish at any finite time for a pure state,  $r = 1$  [19]. On the contrary, any small degree of mixedness leads to disentanglement at a finite time. Note that  $t_{ESD}^{ad}$  depends on the operating points  $\theta_\alpha$ . Here we report the ESD times for identical qubits,  $\Omega_\alpha = \Omega$ ,  $\theta_\alpha = \theta$ , operating at the optimal point ( $\theta = \pi/2$ ) and at pure dephasing ( $\theta = 0$ )

$$t_{ESD}^{ad} = \frac{\Omega}{\Sigma^2} \sqrt{16|ab|^2 \frac{r^2}{(1-r)^2} - 1}, \quad (\theta = \frac{\pi}{2}) \quad (9)$$

$$t_{ESD}^{ad} = \frac{1}{\Sigma} \sqrt{\ln\left[4|ab|\frac{r}{1-r}\right]}, \quad (\theta = 0) \quad (10)$$

where we assumed both qubits affected by the same amplitude  $1/f$  noise,  $\Sigma_\alpha \approx \Sigma$ . The dimensionless ESD time

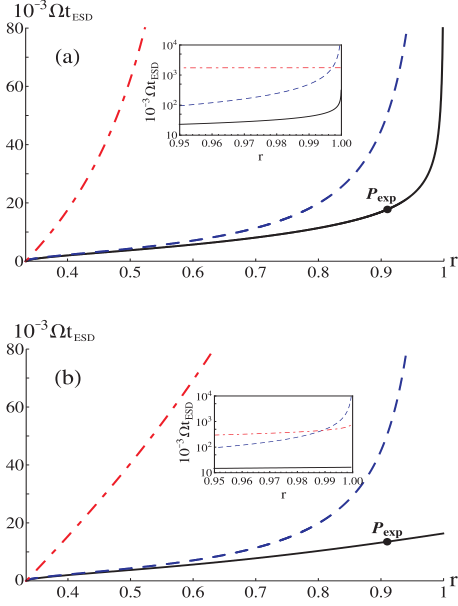


FIG. 2: (Color online) Dependence of the ESD time on the purity  $r$  ( $a = 1/\sqrt{2}$ ) for initial state  $\hat{\rho}^\Phi$  (panel a), and  $\hat{\rho}^\Psi$  (panel b). The blue dashed curve is  $\Omega t_{ESD}^{ad}$ , Eq.(9), red dot-dashed curve is for quantum noise, black curve is the result of adiabatic and quantum noise. Noise characteristics are  $\Sigma = 0.02\Omega$ ,  $S_f(\omega) = 2 \times 10^6 \text{ s}^{-1}$ . In addition,  $\Omega = 10^{11} \text{ rad/s}$ ,  $\theta = \pi/2$ ,  $T = 0.04 \text{ K}$ . The inset zooms the region where  $r \approx 1$ . The point  $P_{exp}$  corresponds to  $r_{exp} \approx 0.91$  where  $\Omega t_{ESD} \approx 18 \times 10^3$  for  $\hat{\rho}^\Phi$  and  $\Omega t_{ESD} \approx 14 \times 10^3$  for  $\hat{\rho}^\Psi$ .

$\Omega t_{ESD}^{ad}$  is longer at the optimal point than for pure dephasing. This is originated from the different (algebraic or exponential) decay of the concurrence Eq. (8) at the two operating points. This behavior, due to the non-Markovian nature of  $1/f$  noise, results in a different scaling of  $\Omega t_{ESD}^{ad}$  with  $\Omega/\Sigma \gg 1$  and in an algebraic or logarithmic (at  $\theta = 0$ ), dependence on  $r$  and  $a$ . The degree of purity of the initial state,  $r$ , has a crucial quantitative role on the ensuing entanglement maintenance. This is illustrated in Fig. 1 for  $1/f$  noise amplitude expected in single qubit experiments  $\Sigma/\Omega = 0.02$  [4, 10, 12]. The dependence on the initial degree of entanglement is instead smoother and symmetric around  $|a|^2 = 1/2$ .

In the multistage approach, quantum noise ( $\omega \sim \Omega$ ) adds up to the defocusing channel leading to extra exponential decay of the coherences and evolutions of the populations. This last fact makes the concurrence of the two EWL states nonequivalent. At finite temperature, quantum noise leads to ESD even for initial Bell-like states ( $r = 1$ ) [15]. This is the main qualitative difference with adiabatic noise. Here we discuss the interplay of adiabatic and quantum noise simultaneously affecting nanodevices. We assume both qubits operate at the optimal point, where the effect of adiabatic noise is reduced.

*Interplay of adiabatic and quantum noise* – The concurrence is evaluated from Eqs. (4) - (5) with qubit  $\alpha$  populations obtained from the Born-Markov master equation. In the presence of white noise at frequencies  $\omega \sim \Omega$ , they read  $\rho_{ii}^\alpha(t) = (\rho_{ii}^\alpha(0) - \rho_{ii}^{\alpha\infty})e^{-t/T_1} + \rho_{ii}^{\alpha\infty}$  with re-

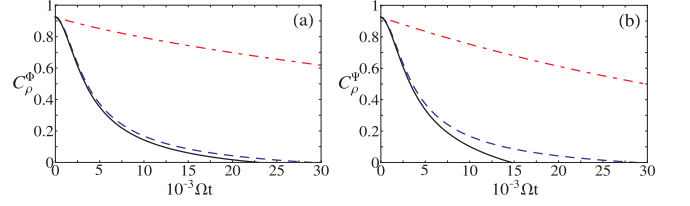


FIG. 3: (Color online)  $C_\rho^\Phi$  (panel a) and  $C_\rho^\Psi$  (panel b) as a function of the dimensionless time  $\Omega t$  for  $r = 0.95$  with  $a = 1/\sqrt{2}$  for adiabatic (blue dashed), quantum (red dot-dashed), and their interplay (black solid). Noise and qubit characteristics as in Fig. 2.

laxation rate  $T_1^{-1} = S_f(\Omega)/2$  and asymptotic population difference  $\rho_{11}^{\alpha\infty} - \rho_{00}^{\alpha\infty} = -\tanh(\Omega_\alpha/2k_B T)$ . The coherences acquire an additional exponential decaying factor,  $T_2^{-1} = T_1^{-1}/2$ , and read

$$\rho_{01}^\alpha(t) \approx \rho_{01}^\alpha(0) e^{-i\Omega_\alpha t - \frac{1}{2} \ln\left(1 + \left(i\Omega_\alpha + \frac{1}{T_1}\right) \frac{\Sigma_\alpha^2 t}{\Omega_\alpha^2}\right) - \frac{t}{2T_1}}. \quad (11)$$

The concurrence can be evaluated in analytic form. Expressions are quite lengthy and here we exemplify the case of initial Bell states ( $r = 1$ ,  $a = 1/\sqrt{2}$ ) and resonant qubits:  $C_\rho^\Phi(t) = 2\max\{0, K_1^\Phi(t)\}$ ,  $C_\rho^\Psi(t) = 2\max\{0, K_2^\Psi(t)\}$  where

$$\begin{aligned} K_1^\Phi(t) &= \frac{1}{2} \frac{e^{-\frac{t}{T_1}}}{\sqrt{1 + \Sigma^4(t/\Omega)^2}} - \sqrt{\rho_{11}^\infty \rho_{00}^\infty} (1 - e^{-\frac{t}{T_1}}) \\ &\times \sqrt{((\rho_{00}^\infty)^2 + (\rho_{11}^\infty)^2) e^{-\frac{t}{T_1}} + \rho_{00}^\infty \rho_{11}^\infty \left(1 + e^{-\frac{2t}{T_1}}\right)} \quad (12) \\ K_2^\Psi(t) &= \frac{1}{2} \frac{e^{-\frac{t}{T_1}}}{\sqrt{1 + \Sigma^4(t/\Omega)^2}} - \frac{1}{2} (1 - e^{-\frac{t}{T_1}}) \\ &\times \left[ ((\rho_{00}^\infty)^2 + (\rho_{11}^\infty)^2) e^{-\frac{t}{T_1}} + 2\rho_{00}^\infty \rho_{11}^\infty \right]. \quad (13) \end{aligned}$$

In general, due to the presence of quantum noise, entanglement is lost in a finite time for any  $r$  and  $a$ . A comparison of the ESD times in the presence of adiabatic noise, quantum noise and their interplay is illustrated in Fig.(2) for white noise level expected from single qubit experiments,  $S_f(\omega) = 2 \times 10^6 \text{ s}^{-1}$  and for the two Werner states. The overall ESD time for states  $\hat{\rho}^\Phi(0)$  is longer than the one for  $\hat{\rho}^\Psi(0)$ . This effect originates from relaxation processes due to quantum noise. The two-excitation state  $|\Psi\rangle$  can decay to a one-excitation state  $|\Phi\rangle$ , while the inverse transition is strongly suppressed at low temperature,  $k_B T \ll \Omega$ . This mechanism does reflect on the evolution of populations appearing in Eq. (4) leading to a faster increase of the population term in  $C_\rho^\Psi(t)$  than in  $C_\rho^\Phi(t)$ , see Eqs. (12) - (13). Note that for high purity levels, the ESD time due to quantum noise is shorter than the adiabatic ESD time (Fig. 2 inset), which goes to infinity for pure states. This observation however has to be supplemented with a quantitative estimate of the amount of entanglement preserved before ESD takes place. Indeed, for typical amplitudes of  $1/f$  and white noise, adiabatic noise considerably reduces the amount of entanglement on a short time scale even for  $r \rightarrow 1$ . This is

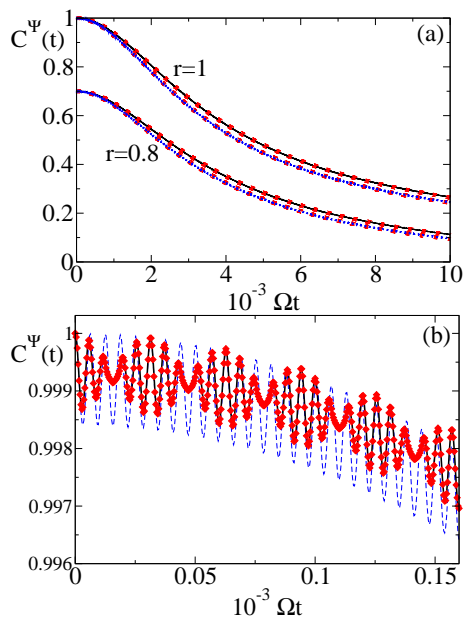


FIG. 4: (Color online)  $C^\Psi(t)$  as a function of the dimensionless time  $\Omega t$  for  $1/f$  noise in  $[1, 10^6]$  Hz, and  $\Sigma/\Omega = 0.02$  at  $\theta = \pi/2$ . Panel (a): detuned qubits  $\Omega_1 (\Omega_2) = 1, (1.2) \times 10^{11}$  rad/s (black), or resonant qubits  $\Omega = \Omega_1$  (dashed blue). Dotted lines are the SPA, Eq. (8). Panel (b): non-resonant qubits with (black) or without (dotted red (gray)) coupling  $\frac{g}{2}\sigma_{z,A} \otimes \sigma_{z,B}$ ,  $g = 10^9$  rad/s. Uncoupled resonant qubits (dashed blue) from numerical simulations.

shown in Fig. 3, where  $C_\rho^\Phi, (C_\rho^\Psi) \approx 1/\sqrt{2}$  (for lower values of concurrence Bell violation always occurs [20]) at  $\Omega t \approx 2.38 \cdot 10^3, (2.24 \cdot 10^3)$ .

*On-chip entanglement generation and maintenance* – In the final part of this Communication we comment on the sensitivity of the above analysis to experimental imperfections and on the possibility to achieve, in a single chip, both entangling (preparation) and local operations. A detuning between the two qubits of about 20% does not change even quantitatively our analysis. This is illustrated in Fig. 4(a) for different initial purity of the Bell-like state  $\rho^\Psi$ . Note that the SPA is reliable even when the dynamics of impurities responsible for  $1/f$  noise extend-

ing up to  $\gamma_M \approx 10^6 \text{ s}^{-1} \ll \Omega_\alpha$  is considered (numerical simulations). Similar effects occur in the presence of a few per-cent deviations around the fixed working point.

In addition, this picture is not modified if detuned qubits are coupled via  $-\frac{g}{2}\sigma_{z,A} \otimes \sigma_{z,B}$ , provided that  $g \ll |\Omega_1 - \Omega_2|, \Omega_\alpha$ . Deviations are visible only on a very small scale, Fig. 4(b). This fact points out that local (single qubit) operations may be performed with detuned qubits even in the presence of a fixed transverse coupling (here we consider  $\theta_\alpha = \pi/2$ ). Tuning the individual qubit splittings on/off resonance effectively switches on/off their interaction. This suggests that entanglement generation and local operations may be performed on-chip in a fixed coupling scheme. Entanglement can be generated by tuning the qubits on resonance. Without modifying the inter-qubit coupling, once induced a detuning, entanglement may be maintained. Both operations take place in the presence of broadband noise and their efficiency depends on the device operating point. The present analysis shows that long - time maintenance of entanglement during local operations can be achieved by operating the two qubits at their own optimal point. In view of the different qualitative behavior of single-qubit and entanglement evolution, this result was not as a priori established. On the other side, it has been recently demonstrated that by properly fixing the qubits coupling strength, high-fidelity two qubit operations can be achieved and entanglement generated [21]. It is therefore possible, depending on the operation, to fix accordingly the optimal operating conditions of the nanodevice. In conclusion, we have studied a physical system where effectively amplitude and phase noise act on a X-state [9]. We demonstrated that even if adiabatic noise may not induce ESD, for typical noise figures, it reduces the amount of entanglement initially generated faster than quantum noise. The main effect of quantum noise consists in differentiating classes of states more or less affected by relaxation processes. In the presence of transverse noise, one-excitation states maintain entanglement longer than two-excitation states. Efficiency of entanglement preservation sensitively depends on the initial state purity.

[1] Y. Nakamura *et al.*, Nature **398**, 786 (1999); Y. Yu *et al.*, Science **296**, 889 (2002); J.M. Martinis *et al.*, Phys. Rev. Lett. **89**, 117901 (2002); I. Chiorescu *et al.*, Science, **299**, 1869, (2003); T. Yamamoto *et al.*, Nature **425**, 941 (2003); S. Saito *et al.*, Phys. Rev. Lett. **93**, 037001 (2004); J. Johansson *et al.*, *ibid.* **96**, 127006 (2006); F. Deppe *et al.*, Nature Phys. **4**, 686 (2008).  
[2] E. Lucero *et al.*, Phys. Rev. Lett. **100**, 247001 (2008); J. M. Chow *et al.*, Phys. Rev. Lett. **102**, 090502 (2009).  
[3] J. A. Schreier *et al.*, Phys. Rev. B **77**, 180502(R) (2008).  
[4] D. Vion *et al.*, Science **296**, 886 (2002).  
[5] Yu. A. Pashkin *et al.*, Nature **421**, 823 (2003); A. J. Berkley *et al.*, Science **300**, 1548 (2003); T. Yamamoto

*et al.*, Nature **425**, 941 (2003); A. Izmailkov *et al.*, Phys. Rev. Lett. **93**, 037003 (2004); J. B. Majer *et al.*, Phys. Rev. Lett. **94**, 090501 (2005); T. Hime *et al.*, Science **314**, 1427 (2006); A. O. Niskanen *et al.*, Science **316**, 723 (2007); J. Majer *et al.*, Nature **449**, 443 (2007); S. H. W. van der Ploeg *et al.*, Phys. Rev. Lett. **98**, 057004 (2007); A. Fay *et al.*, *ibid.* **100**, 187003 (2008).  
[6] M. Steffen *et al.*, Science **313**, 1423 (2006). J.H. Plantenberg *et al.*, Nature **447**, 836 (2007); S. Filipp *et al.*, Phys. Rev. Lett. **102**, 200402 (2009); P. J. Leek *et al.*, Phys. Rev. B **79**, 180511(R) (2009).  
[7] L. DiCarlo *et al.*, Nature **460**, 240 (2009).  
[8] M. Nielsen and I. Chuang, *Quantum Computation and*

*Quantum Information* (Cambridge Univ. Press, 2005).

- [9] T. Yu, J. H. Eberly, *Science* **323**, 598 (2009).
- [10] G. Ithier *et al.*, *Phys. Rev. B* **72**, 134519 (2005).
- [11] O. Astafiev *et al.*, *Phys. Rev. Lett.* **93**, 267007 (2004).
- [12] G. Falci *et al.*, *Phys. Rev. Lett.* **94**, 167002 (2005).
- [13] T. Yu, J. H. Eberly, *Phys. Rev. Lett.* **93**, 140404 (2004).
- [14] B. Bellomo *et al.* *Phys. Rev. Lett.* **99**, 160502 (2007).
- [15] B. Bellomo *et al.* *Phys. Rev. A* **78**, 060302(R) (2008).
- [16] Correlated noise and cross-talk effects addressed in A. D'Arrigo *et al.*, *New J. Phys.* **10**, 115006 (2008).
- [17] W. K. Wootters, *Phys. Rev. Lett.* **80**, 2245 (1998).
- [18] M. B. Weissman, *Rev. Mod. Phys.* **60**, 537 (1988).
- [19] T. Yu and J. H. Eberly, *Quant. Inf. Comp.* **7**, 459 (2007).
- [20] F. Verstraete and M. M. Wolf, *Phys. Rev. Lett.* **89**, 170401 (2002).
- [21] E. Paladino *et al.*, *Phys. Rev. B* **81**, 052502 (2010).